A Numerical Study on Buckling for Thin Shell Structures Made of Rubber

Hiroshi Kurimoto, Makoto Saito, Ph.D.

CAE & Materials Department, Nabtesco Corporation, Japan

Abstract: Thin shell structures made of rubber are often used to protect sliding areas from dust and water. Though they can respond to large scale deformation, cracking happens when buckling distortion with sharp curvatures occurs. Therefore, predicting buckling is vital for the design of these thin shell structures.

In this paper, three kinds of nonlinear static analyses (nlgeom, nlgeom with automatic stabilization options, and the Riks method) and three kinds of dynamic analyses (Explicit, Implicit with transient fidelity and Implicit with quasi-static) were carried out on a thin shell structure which showed obvious buckling in experiments. While no buckling deformation mode was observed in any of the static analyses, the buckling deformation mode observed in the experiment was precisely simulated throughout the buckling event without any geometric imperfection in all the dynamic analyses. In addition, the critical stroke and reaction force of the buckling in the dynamic analyses were in good agreement with the experimental results. Parametric analyses results will be presented and discussed.

Keywords: Experimental Verification, Rubber, Buckling, Shell Structures, Static Analysis, Dynamic Analysis

1. Introduction

To estimate critical loads and reliability against buckling, the eigenvalue buckling analysis is a common and useful approach. But this eigenvalue buckling analysis is a linear analysis, so it is difficult to predict buckling deformation accurately. Especially, in the case of the buckling of thin cylindrical shell structures, the eigenvalue buckling analysis produces many buckling modes near the critical load point. But in the real buckling process, only a few buckling modes of the many buckling modes predicted actually occur.

Furthermore, for the design of thin shell structures made of rubber, it is important to predict buckling deformation and post-buckling behavior accurately, because failure of the material depends on stress and strain under buckling deformation.

So in this paper, several approaches were implemented to predict buckling deformation and post-buckling behavior accurately, and the results were compared with experimental results.

2. Analytical methods

2.1 Analytical object and boundary conditions

The analytical object described in this paper is a cylindrical shell structures made of rubber. Figure 1 is a cross section of the analytical object. The area indicated by a blue line in Figure 1 is connected to a base (blue dotted line) that is fixed, and the red line area is fixed on a rod (red dotted line) that has a prescribed displacement of 30mm. The shell protects the sliding area from dust and water.

In this analysis, the blue line area was fixed, and a downward prescribed displacement stroke of 30 mm was applied on the red line area.

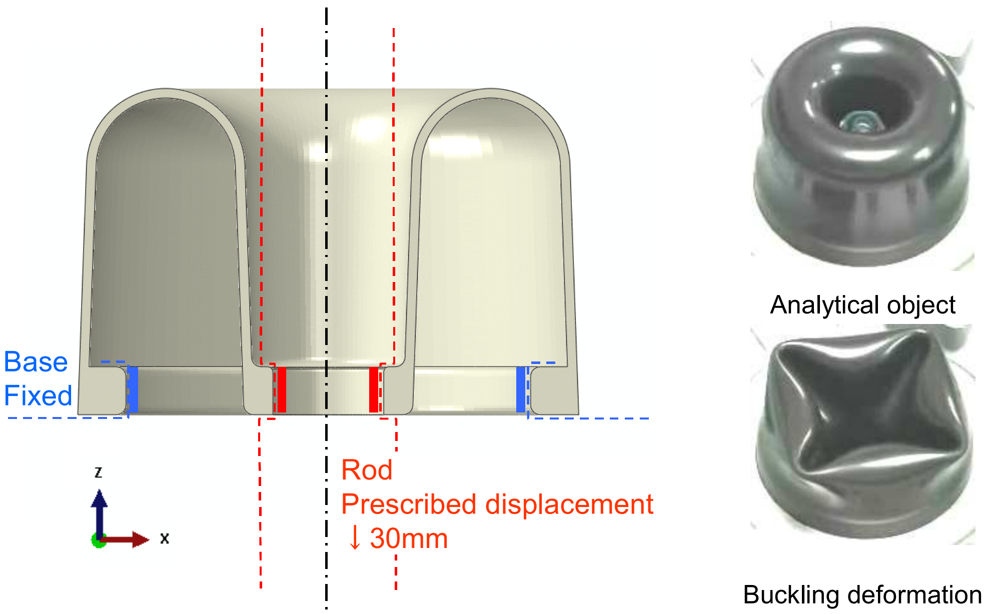

Figure 1. Analytical object and boundary conditions

2.2 Properties of material

This analytical object is made of rubber, so the neo-Hookean strain energy potential was selected to create response curves automatically and to evaluate the hyperelastic material behavior. Two parameters were defined from the shore hardness of the material, C_{10} is 0.375, D_1 is 0.133.

2.3 Analysis procedures

Several analysis procedures were carried out to evaluate buckling deformation and behavior. Table 1 gives an overview of the procedures. Three types of nonlinear static analyses were performed; the nlgeom option, nlgeom combined with static stabilizing and (artificial) damping and a modified Riks method (arc-length method). Three kinds of dynamic analyses; Explicit, Implicit with transient fidelity option, and Implicit with the quasi-static option, were carried out.

In these analyses, contact wasn't considered, because preliminary analysis showed that contact does not occur.

Table 1. Analysis procedures

Procedure	Option
Static	Nlgeom
Static	Nlgeom, Stabilize
Static	Nlgeom, Riks
Dynamic Explicit	-
Dynamic Implicit	Transient Fidelity
Dynamic Implicit	Quasi-Static

2.4 Software version

Abaqus version 6.10, with improved dynamic Implicit function, was used as the solver and Abaqus/CAE version 6.10 was used in both pre and post-processing.

3. Measurement

3.1 Measurement method

In this paper, analysis results were compared with verification tests. The verification tests were performed using a fatigue testing machine under the same conditions as the analyses. Images of the buckling behavior were taken, and the stroke and reaction force were measured.

3.2 Results

Figure 2 shows the reaction force-stroke curve and deformations in the verification tests. The results indicate the following features.

i. With less than a 10 mm stroke, the reaction force increases linearly, and no buckling deformation occurs (Figure 2-a).

ii. At approximately 10 mm, buckling occurs at four locations along the circumferential direction, and the inflection point was confirmed in the reaction force-stroke curve (Figure 2-b).

iii. After buckling (10 mm), the reaction force decreased slightly and the slope increased slightly from about 17mm.

iv. The buckling deformation continued through the end of the stroke (Figure 2-c).

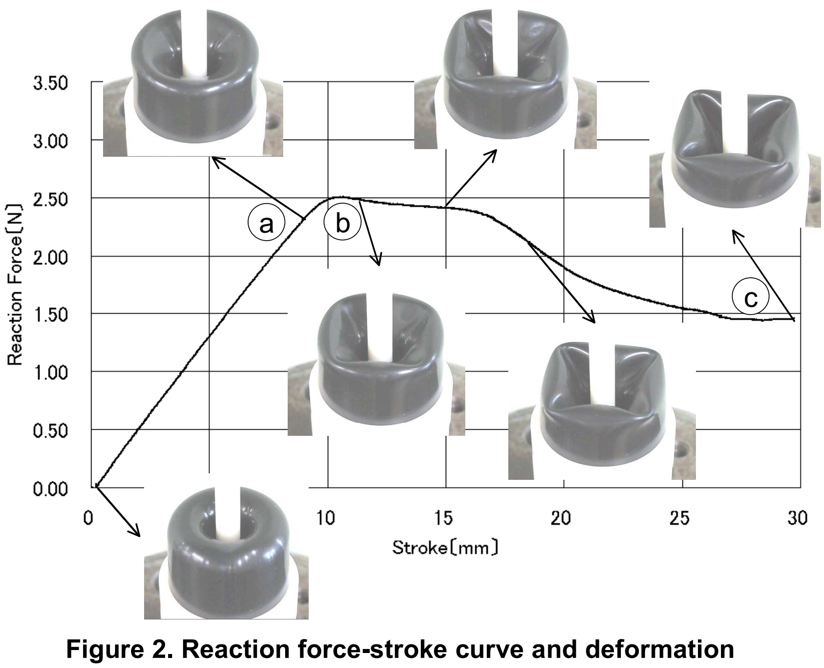

Figure 2. Reaction force-stroke curve and deformation

4. Analysis results and discussion

4.1 Nonlinear static analysis

The reaction force-stroke curve and the deformation of the nonlinear static analyses results are illustrated in Figure 3. All results of the nonlinear static analyses indicate the same tendencies. The reaction force increases linearly in the same manner as the measurement with less than a 10 mm stroke, but buckling deformation doesn't occur around 10 mm when the buckling occurred in the actual test (Figure 3-a). At about 18 mm strokes, there is an inflection point in the reaction force-stroke curve, but the deformation mode doesn't change. No buckling deformation occurs until the end of the stroke.

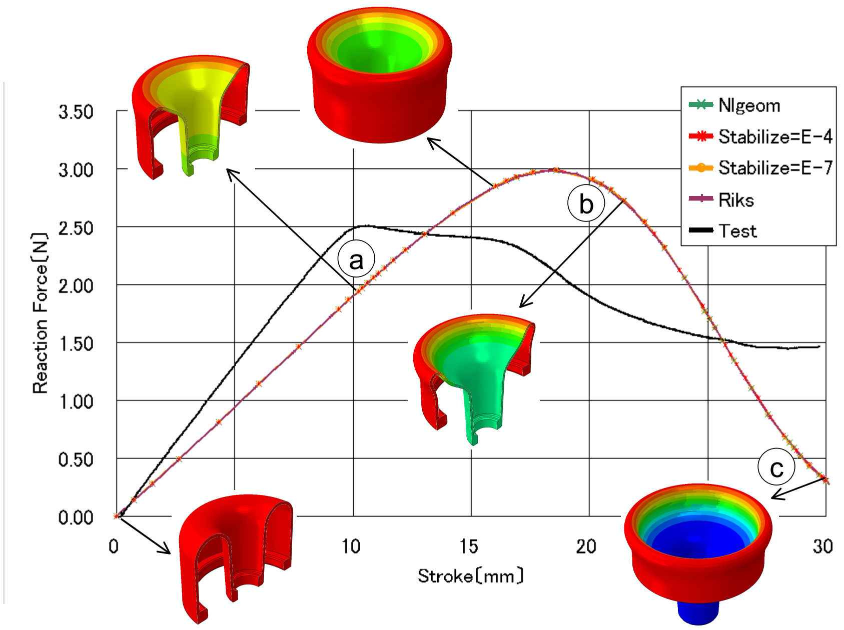

Figure 3. Reaction force-stroke and deformations of nonlinear static analysis

(Contour shows displacement)

4.2 Dynamic Explicit

Figure 4 shows the analysis results of dynamic Explicit. In the analysis, the same buckling behavior as the measurement results was confirmed. The results indicate the following features:

i. Buckling occurred at about 12 mm similar to the measurement results (Figure 4-a).

ii. Buckling deformation occurred at four locations; also in good agreement with the measurements results.

iii. After buckling, short period oscillations occurred which weren't confirmed in the measurement results (Figure 4-b)

iv. The reaction force increased slightly after buckling and from 17mm, it decreased like the measurement results.

The short period oscillations are thought to be caused by the high-frequency vibrations peculiar to dynamic analysis at the start of the buckling deformation.

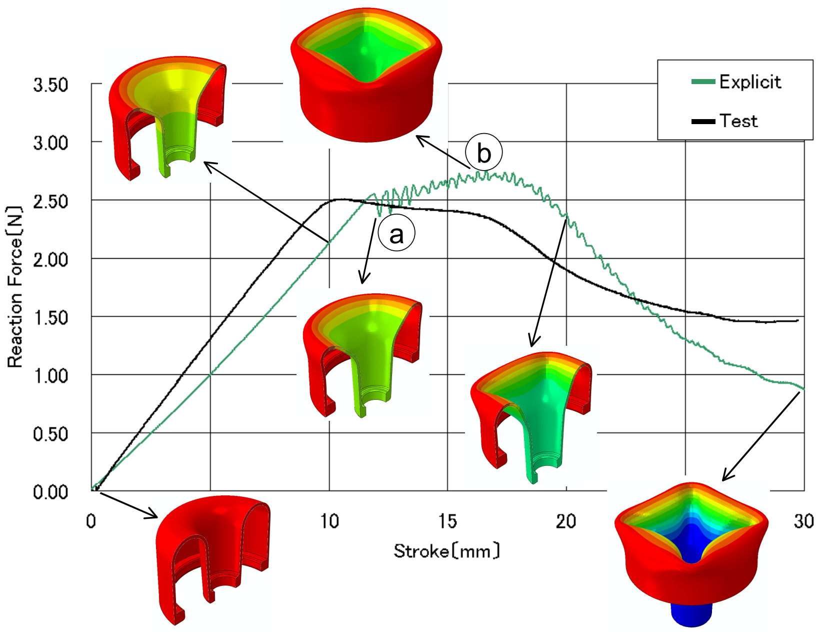

Figure 4. Reaction force-stroke and deformations of dynamic Explicit analysis

(Contour shows displacement)

4.3 Dynamic Implicit

The reaction force-stroke curve and the deformation of the dynamic Implicit analyses results are illustrated in Figure 5. The analysis results of Implicit indicate the same tendencies as the Explicit analysis. The notable difference is that the short period oscillations were dampened earlier. It is thought that the inertia effect described in the user's manual worked to ameliorate the unstable behavior.

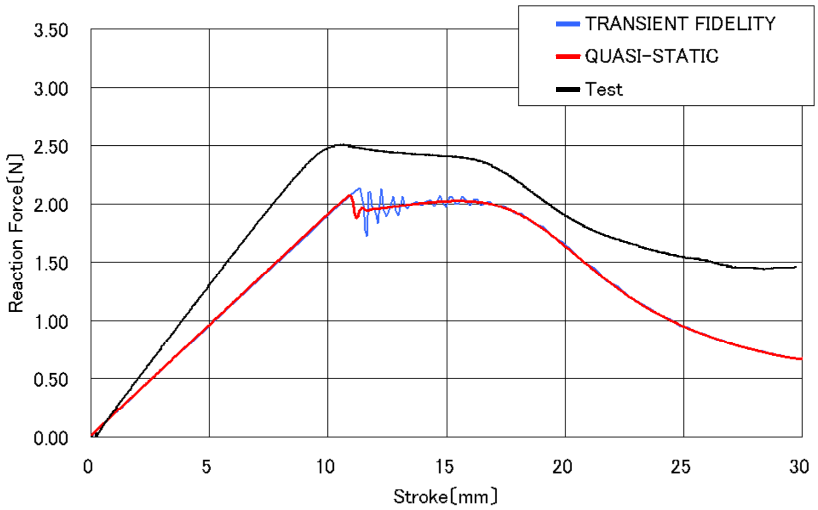

Figure 5. Reaction force-stroke and deformations of dynamic Implicit analyses

4.4 Difference between Explicit and Implicit

Figure 6 shows the reaction force-stroke of the test and several analysis results. With less than a 10 mm stroke before buckling occurs and while the reaction force increases linearly, the slope of Explicit analysis is steeper than that of the other analyses, though the same material parameters were used in all analyses. The historical output of energy in Explicit and Implicit is illustrated in Figure 7. It is clear that the strain energies of both Explicit and Implicit are the same, but the artificial strain energy of Explicit is higher than that of Implicit. In these analyses, the enhanced hourglass control approach was applied. It is thought that this artificial strain energy for hourglass controls increased and the rigidity of the Explicit analysis also increased.

On the other hand, the slope of the analysis results are more gradual than the measurement results. The probable explanation for this is that the material parameters used in these analyses were converted from the shore hardness without testing. The nominal shore hardness and shape values (especially the thickness) used in the design drawing, were used in the analyses.

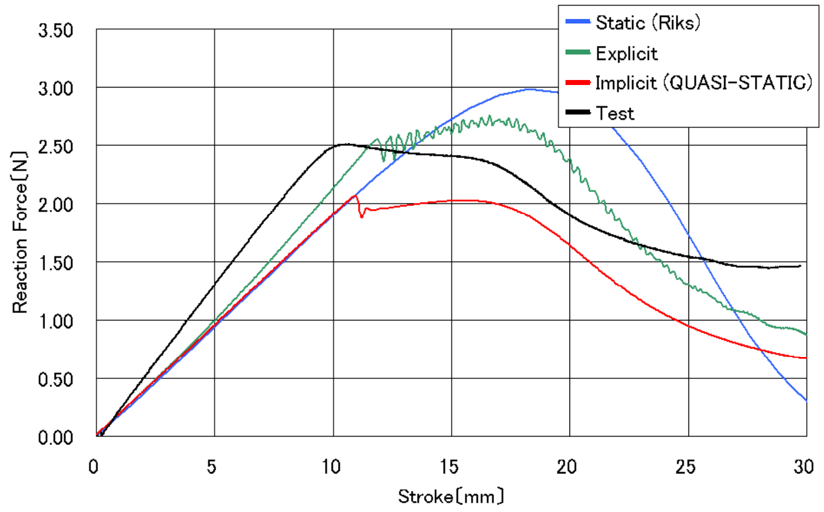

Figure 6. Difference of rigidity

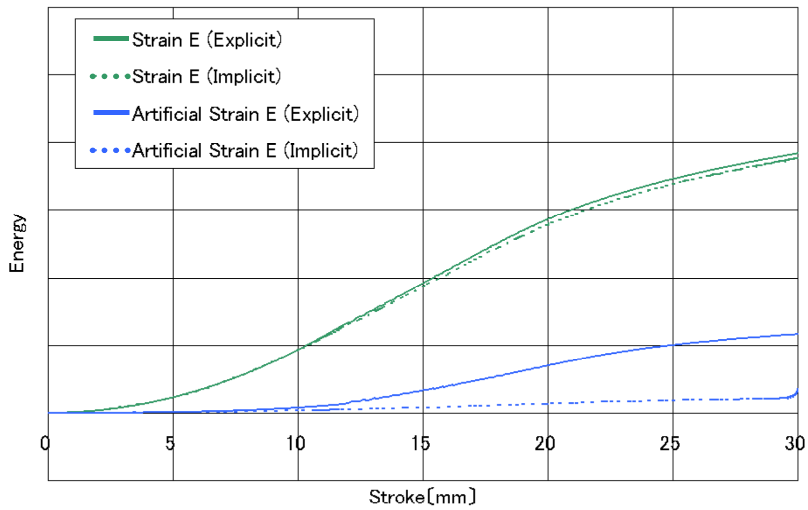

Figure 7. Energy historical output of Explicit and Implicit analysis

4.5 Sudden change of strain

The analysis results show a large difference in behavior between static analysis and dynamic analysis. In the static analyses, buckling deformation didn't occur. On the other hand, in all dynamic analyses, the critical buckling stroke and deformation were in good agreement with test results.

Figure 8 shows the reaction force-stroke curve and circumference strain curve of the Explicit analysis. Though we couldn't confirm any notable change except the high-frequency vibration peculiar to dynamic analysis, the circumference strain changes from compressive to tensile as the curvature reverses. This strain behavior is often seen in "Snap-Through" buckling and is unstable. It is thought that this instability is the reason that static analysis couldn't analyze the buckling behavior successfully.

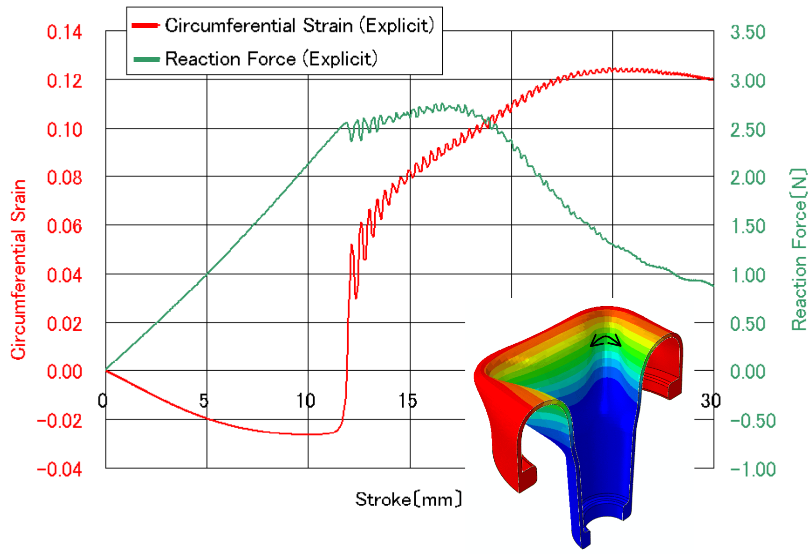

Figure 8. Reaction force and circumferential strain-stroke curve in Explicit analysis

4.6 Eigenvalue buckling

Table 2 indicates the results of the eigenvalue analysis. In this paper, positive geometric and loading imperfections were not considered. Static analysis was not able to analyze buckling successfully, so the eigenvalue buckling was confirmed. It is clear that the four location buckling confirmed in the tests and dynamic analyses occurs at number 22 and 23 and many other buckling modes were identified. It is thought that this is one of the reasons that static analysis couldn't analyze the buckling behavior successfully.

Table 2. Eigenvalue buckling (Input force is 0.01N)

No.	Eigenvalue	Mode	No.	Eigenvalue	Mode
1	241	2	16	306	13
2	241		17	306	
3	282	10	18	308	7
4	282		19	308	
5	283	9	20	320	14
6	283		21	320	
7	286	11	**22**	**333**	**4**
8	286		**23**	**333**	
9	287	3	24	335	6
10	287		25	335	
11	292	8	26	338	15
12	292		27	338	
13	294	12	28	357	16
14	294		29	357	
15	299	0	30	362	5

5. Conclusions

The buckling behavior of a thin cylindrical shell structure made of rubber was carried out using several analysis approaches, and the analysis results were compared with verification tests. The comparative result lead to the following conclusions.

i. Using several nonlinear static analyses, nlgeom, nlgeom with automatic stabilization options, and the Riks method, buckling deformation that was confirmed by the measurements didn’t occur.
ii. Using dynamic analysis, Explicit and Implicit, buckling deformation and critical stroke were in good agreement with the verification tests.
iii. Dynamic analysis can be useful for designing thin shell structures made of rubber that require predicting buckling deformation and post-buckling behavior accurately.

6. Acknowledgements

This paper has been organized based on the contents of a paper presented at the 2010 Simulia Customer Conference Japan held on November 1-2. The authors would like to take this opportunity to thank the support members of Simulia Japan for their assistance.